Tectonophysics 629 (2014) 75–86

Contents lists available at ScienceDirect

Tectonophysics

journal homepage: www.elsevier.com/locate/tecto

On the reliability of the AMS ellipsoid by statistical methods

S. Guerrero-Suarez *, F. Martín-Hernández

Departamento de Física de la Tierra, Astronomía y Astrofísica I, Universidad Complutense de Madrid, 28040 Madrid, Spain
Instituto de Geociencias (UCM,CSIC), Facultad de Ciencias Físicas, 28040 Madrid, Spain

ARTICLE INFO

Article history:
Received 1 October 2013
Received in revised form 2 March 2014
Accepted 6 April 2014
Available online 18 April 2014

Keywords:
Anisotropy of Magnetic Susceptibility
Bootstrap
Linear Perturbation Analysis
Rock magnetism

ABSTRACT

Weak magnetic materials whose susceptibility values are close to the instrument's accuracy show very large errors in the direct evaluation of their ellipsoid parameters. This may lead to misinterpretation of the magnetic fabric, which is often used as a geological indicator. In order to estimate the measurement uncertainties, several statistical methods have been proposed. Within the available statistical methods, the Linear Perturbation Analysis (Hext, 1963) and the non-parametric bootstrap (Constable and Tauxe, 1990) technique have been widely used. In this paper, we make a complete study about these methods to estimate their limitations when applied to n measurements of a single sample. We will analyze which method is better in terms of uncertainties, we will determine when the methods do not provide reliable results and we will establish a measuring protocol. For that, we run simulations for the Linear Perturbation Analysis and the non-parametric bootstrap varying i) the number of measurements, ii) the instrumental error and iii) the shape parameter and the anisotropy degree of the AMS ellipsoid. The results show that both methods are not reliable when the difference between eigenvalues is too close in relation to the instrumental error, but increasing the number of measurements can improve the results.

1. Introduction

The Anisotropy of Magnetic Susceptibility (AMS) is the intrinsic property of a material that describes the directional variability of the induced magnetization with respect to the applied field. In single crystal specimens, the AMS is related to the crystallographic structure according to Neumann's law (Borradaile, 2003). In polycrystalline specimens, the AMS is determined also by the degree of alignment of their constituent crystallites. The alignment is caused by geological processes in almost all rock types. The water flow in sediments (Hamilton and Rees, 1970), the lava or magmatic flow in volcanic and pluton rocks (Cañón-Tapia et al., 1995; Ernst and Baragar, 1992) or the ductile deformation in metamorphic rocks (Hrouda, 1993) are some of the principal processes studied by means of AMS measurements. Because of this, since mid-1970s, the AMS studies have been an important tool in structural geology, petrofabrics and in the interpretation of magnetic fabrics (Borradaile and Henry, 1997; Borradaile and Jackson, 2010; Kodama, 1995; Rochette et al., 1992; Tarling and Hrouda, 1993).

The magnetic susceptibility is linear for diamagnetic minerals by definition. For paramagnetic minerals it is also linear for most available magnetic fields. For ferromagnetic minerals, however, there is a weak field range for which the susceptibility can be considered linear and fitted mathematically into a second rank tensor, that is, a 3×3 symmetric matrix $\mathbf{K}$ such that $\mathbf{M} = \mathbf{KH}$ (Dunlop and Özdemir, 2001). Most ferromagnetic minerals show this linear behavior for fields under 0.1 mT (Hrouda, 2002). The typical way to characterize the anisotropy is to calculate the eigenvalues and the orthogonal eigenvectors of the susceptibility tensor and its graphical representation.

The usual experimental procedure to calculate the susceptibility matrix consists of measuring bulk susceptibilities along several known directions. Different experimental protocols (sets of directions to measure along) have been proposed; for a revision, see Borradaile (2003) and references therein. The first schemes included six orientations; however, later works increased the number of positions in order to include an estimation of the error in the mathematical fitting of the susceptibility tensor. A 7-orientation scheme and a 13-orientation scheme were proposed by Borradaile and Stupavsky (Borradaile and Stupavsky, 1995). Both schemes, 7- and 13-orientation, are used in Sapphire Instruments equipment. The KLY series and later MFK devices from AGICO Instruments use however the 15-orientation scheme proposed by Jelinek (1977). More schemes were discussed by Hext (1963) and Jelínek (1978) but did not become popularly used.

In order to get a complete AMS analysis from the orientation schemes, it is recommended an estimation of the confidence intervals for the eigenvalues and the confidence ellipses for the eigenvectors. The readings of bulk susceptibility, or data $\mathbf{d}$, can be expressed as

$$\mathbf{d} = \mathbf{Dk} + \mathbf{e} \tag{1.1}$$

where:

- $\mathbf{D}$ is the experimental design-matrix, the matrix of directional cosines of the orientation scheme,

* Corresponding author.
E-mail address: saguerre@ucm.es (S. Guerrero-Suarez).

http://dx.doi.org/10.1016/j.tecto.2014.04.010
0040-1951/

- **k** is the column vector with the six independent elements of the susceptibility tensor

$$\mathbf{k} = (\mathbf{K}_{11}, \mathbf{K}_{22}, \mathbf{K}_{33}, \mathbf{K}_{12}, \mathbf{K}_{23}, \mathbf{K}_{13})^{\mathbf{T}} \tag{1.2}$$

- **e** is a column vector of random errors.

The best-fit for the susceptibility tensor is the result of multiplying the data (**d**) by the generalized inverse of matrix **D**:

$$\overline{\mathbf{k}} = \left(\mathbf{D}^{\mathbf{T}}\mathbf{D}\right)^{-1}\mathbf{D}^{\mathbf{T}}\mathbf{d}. \tag{1.3}$$

Two different statistical methods are the most popular to estimate the confidence intervals of the susceptibility tensor: Linear Perturbation Analysis (LPA) (Hext, 1963; Jelínek, 1978) and non-parametric bootstrap (NPB) (Constable and Tauxe, 1990).

In the LPA method, the mean tensor for a number n of specimens (or number n of measurements of one specimen) is calculated by the theory of least squares fitting. To estimate the confidence intervals of the eigenparameters, the errors **e** are assumed small, independent and normally distributed. To calculate the confidence ellipses, the eigenvector distribution is assumed to be a two-dimensional normal distribution with semi-axes aligned along the mean eigenvectors.

Bootstrap analysis has two approaches: parametric bootstrap and non-parametric bootstrap. The difference lies in the assumptions on the data distribution. The parametric bootstrap assumes a particular data distribution and the non-parametric bootstrap does not (Davison, 1997).

The non-parametric bootstrap analysis is a random re-sampling method with replacement of observations from the original sample. It allows estimating standard errors, bias and confidence intervals for the parameters. In particular, the bootstrap analysis proposed by Constable and Tauxe (1990), a widely used method and associated software used in the paleomagnetic community (Tauxe, 2010), is a non-parametric bootstrap. The mean tensor is calculated in the same way than for the LPA method. To calculate the confidence ellipse, the eigenvector distribution is assumed to be a Kent distribution (also known as Fisher–Bingham 5 distribution).

The problem of the two methods, LPA and NPB, is that both could yield unrealistic results. They strongly depend on the ratio of the instrumental error to the bulk susceptibility, and the ratio of the instrumental error to the differences between eigenvalues. The AMS of a magnetically weak sample, like one of quartz single crystal with $k_{bulk} \sim 10^{-5}$ [SI] (Tarling and Hrouda, 1993), and an anisotropically weak sample, such as one of calcite with $\lambda_{max} - \lambda_{min} \sim 10^{-6}$ [SI] (Schmidt et al., 2006) may not be well-determined. A magnetically weak sample is defined here as a sample whose bulk susceptibility value is close to the instrumental error. An anisotropically weak sample is one for which the differences between its susceptibility eigenvalues lie within the range of the instrumental error.

The instrumental error includes, together with the technical sensitivity, other sources such as thermal drift and/or mechanical drift. These additional sources increase the instrumental error at least one order of magnitude with respect to its technical sensitivity (Biedermann et al., 2013). The sensitivity of the most common commercial instruments is in the range from 10^{-6} [SI] for Sapphire Instruments susceptibility bridge (Borradaile et al., 2008) and Bartington MS2/MS3 (www.bartington.com) to 10^{-8} [SI] for AGICO Instruments (Hrouda and Pokorný, 2011).

Both methods (LPA and NPB) have been compared in previous works (Borradaile, 2003; Owens, 2000a; Owens, 2000b; Werner, 1997) for the case of multiple specimens. The main differences found are the size and orientation of the semiaxes of the confidence ellipses.

The goal of this study is to show how the reliability of the LPA and the NPB methods varies according to the instrumental error, the magnitude of the bulk susceptibility and the difference between the eigenvalues. Moreover we will establish validity limits for both methods and a protocol of measure for the case of n measurements of a single specimen.

In order to estimate the reliability, we will check if the success rate reaches the confidence level used in the LPA and the NPB methods. The success rate is the probability for the real anisotropy tensor lying inside the estimated confidence intervals. We estimate this probability by performing 500 simulations of the calculation of the AMS ellipsoid. We study the reliability for different cases of magnetically and anisotropically weak samples with different instrumental errors and number of measurements.

2. Methodology

We have used a reference tensor, called the real tensor, to check the reliability. The synthetic data used to run the simulations will be generated from this real tensor and a known error distribution. In each simulation, the LPA and the NPB methods will be used to obtain the AMS eigenparameters and their confidence intervals. For the eigenvectors, the confidence regions are spherical ellipses, whose major and minor semiangles are called η and ζ respectively. We will use the reference tensor to estimate the success rate of both methods.

2.1. Synthetic data

The synthetic data are represented as a column vector that contains all measurements of the different positions of the chosen scheme. In this work, we have generated synthetic data for a 15-orientation scheme (Jelinek, 1977), typical of AGICO Instruments. In order to create this vector, the following parameters are necessary:

- $\mathbf{K}_{real}$: the real tensor, from which we can obtain the three eigenvalues ($\lambda_1, \lambda_2, \lambda_3$) and their eigenvectors ($\mathbf{v}_1, \mathbf{v}_2, \mathbf{v}_3$). The eigenvalues determine the mean susceptibility defined as $\lambda_{mean} = (\lambda_1 + \lambda_2 + \lambda_3)/3$, the degree of anisotropy (P) and the shape parameter (U) of the ellipsoid. The anisotropy degree is defined as $P = \lambda_1/\lambda_3$ (Nagata, 1961) and the shape parameter as $U = \frac{2\lambda_2 - \lambda_1 - \lambda_3}{\lambda_1 - \lambda_3}$ (Jelinek, 1981). These two variables (P and U) indicate how the spacing between the eigenvalues is distributed.
- **D**: the design-matrix that contains the directional cosines of the 15-orientation scheme.
- σ: the standard deviation of the instrumental error distribution assuming it follows a normal distribution (Biedermann et al., 2013). Experimentally, the instrumental error cannot be modified, but in this work, σ has been included in the simulations as the percentage of the mean susceptibility λ_{mean}. That is, a σ value of 0.1 would mean an instrumental error of 10% of λ_{mean}. This parameter indicates how magnetically weak the data are.

The real vector that will contain the 15-orientation measures is calculated from the real tensor and the design-matrix as

$$\mathbf{d}_{real} = \mathbf{D}\mathbf{K}_{real}, \tag{2.1}$$

where the design matrix is

$$\mathbf{D} = \begin{pmatrix} .5 & .5 & 0 & -1 & 0 & 0 \\ .5 & .5 & 0 & 1 & 0 & 0 \\ 1 & 0 & 0 & 0 & 0 & 0 \\ .5 & .5 & 0 & -1 & 0 & 0 \\ .5 & .5 & 0 & 1 & 0 & 0 \\ 0 & .5 & .5 & 0 & -1 & 0 \\ 0 & .5 & .5 & 0 & 1 & 0 \\ 0 & 1 & 0 & 0 & 0 & 0 \\ 0 & .5 & .5 & 0 & -1 & 0 \\ 0 & .5 & .5 & 0 & 1 & 0 \\ .5 & 0 & .5 & 0 & 0 & -1 \\ .5 & 0 & .5 & 0 & 0 & 1 \\ 0 & 0 & 1 & 0 & 0 & 0 \\ .5 & 0 & .5 & 0 & 0 & -1 \\ .5 & 0 & .5 & 0 & 0 & 1 \end{pmatrix} \tag{2.2}$$

and $\mathbf{k}_{real}$ is the vector with the six independent components of the real susceptibility tensor $\mathbf{K}_{real}$, as in Eq. (1.2).

The known error distribution is used to calculate n simulated measures for each 15 positions (Jelinek, 1977) and to introduce the instrumental error in the real measures ($\mathbf{d}_{real}$). Then, the synthetic vector used to run the simulations will be calculated from a normal distribution with mean $\mu = \mathbf{d}_{real;i}$, where $\mathbf{d}_{real;i}$ is the real value for the position i, and standard deviation σ.

2.2. Linear Perturbation Analysis: Hext method

According to Hext (1963) the mean susceptibility tensor is calculated from Eq. (1.3) and the errors $\mathbf{e}$ in Eq. (1.1) are assumed random, independent and normally distributed. The confidence intervals for the eigenparameters at the 95% confidence level are calculated in the following way:

- For the eigenvalues,

$$\lambda_{i,Hext} \pm t_{(1-\alpha/2)}\left(n^{-1}\sigma\mathbf{a}_{ii}^{\mathbf{T}}\left(\mathbf{D}^{\mathbf{T}}\mathbf{D}\right)^{-1}\mathbf{a}_{ii}\right)^{1/2},$$

where t is the Student's t-distribution for n degrees of freedom, and $\mathbf{a}_{ij}$ is a function of the unit vectors $\mathbf{X}_i$, $\mathbf{X}_j$ such that $\mathbf{X}_i^{\mathbf{T}}\mathbf{S}\mathbf{X}_j = \mathbf{a}_{ij}\mathbf{s}$ for any symmetric matrix $\mathbf{S}$ for which $\mathbf{s}$ is the six component vector representation (Eq. (1.2)). The estimated variance is

$$\sigma = \sqrt{\frac{\sum \mathbf{e}_i^2}{n_f}},$$

where $n_f = N - 6$ is the number of degrees of freedom, in the case of n measures and a design of 15 positions, $N = 15n$, and $\mathbf{e}_i = \mathbf{d}_i - \mathbf{D}_{ij}\overline{\mathbf{k}}_j$ are the residuals.

- For the eigenvectors ($\mathbf{v}_i$), the confidence regions are ellipses whose semi-angles are aligned with the eigenvectors. The semiangles are calculated by

$$\begin{aligned}
\epsilon_{12} &= \tan^{-1}(f\sigma/2(\lambda_1 - \lambda_2)) \\
\epsilon_{23} &= \tan^{-1}(f\sigma/2(\lambda_2 - \lambda_3)) \\
\epsilon_{13} &= \tan^{-1}(f\sigma/2(\lambda_1 - \lambda_3)) \\
\epsilon_{21} &= \epsilon_{12} \\
\epsilon_{32} &= \epsilon_{23} \\
\epsilon_{31} &= \epsilon_{13},
\end{aligned} \tag{2.3}$$

where ϵ_{ij} defines the semiaxis directed towards $\mathbf{v}_j$ for the confidence region of $\mathbf{v}_i$, and $f = \sqrt{2\left(F_{(2,n_f);(1-\alpha)}\right)}$, being $F_{(2,n_f);(1-\alpha)}$ the $1-\alpha$ quantile of the F distribution with 2 and n_f degrees of freedom. For more details, see Hext (1963).

In order to make the nomenclature consistent, $\eta_1 = max(\epsilon_{12}, \epsilon_{13})$, and $\zeta_1 = min(\epsilon_{12}, \epsilon_{13})$. In the same way, we will rename the semiaxis η_2, ζ_2, η_3 and ζ_3.

2.3. Non-parametric bootstrap method

The bootstrap method introduced by Constable and Tauxe (1990) is a non-parametric bootstrap which consists of the following steps:

1. Compute the $\mathbf{K}_j$ ($j = 1 \ldots n$) from Eqs. (1.3) and (1.2).[1]
2. Compute a pseudo-mean tensor $\overline{\mathbf{K}} = n^{-1}\sum_{i=1}^{n}\hat{\mathbf{K}}_i$, where $\hat{\mathbf{K}}_i$ ($i = 1 \ldots n$) are randomly selected from the n initial tensors $\mathbf{K}_j$ (re-sampling with replacement).
3. Calculate the eigenparameters for $\overline{\mathbf{K}}$.
4. Repeat N_b times the first three steps to obtain samples of the distributions of each of the eigenparameters.

[1] Usually the next step is normalize $\mathbf{K}_j$ by its trace, but in this paper we do not normalize the tensor because the study is for only one sample measured n-times.

We have used $N_b = 1000$ for the number of iterations of the method.

The mean eigenparameters will be calculated from $\overline{\mathbf{K}}_{mean} = N_b^{-1}\sum_{l=1}^{N_b}\overline{\mathbf{K}}_l$. And the confidence intervals for α confidence level are calculated assuming a normal distribution for each of the eigenvalues, and a Kent distribution for each of the eigenvectors, also called Fisher–Bingham 5 distribution (Kent, 1982). The details on the calculation of the confidence ellipse for the Kent distribution are given in Appendix A.

An important characteristic of the Kent distribution is that, when calculating the confidence ellipse from a set of vectors, the result changes if any of the vectors is exchanged by its opposite. However, if $\mathbf{v}$ is an eigenvector, its opposite $-\mathbf{v}$ is an equally valid eigenvector. Because of this, the directions of the eigenvectors must be carefully chosen before calculating the corresponding confidence ellipse. In this paper, our selection criterion is the minimum angular distance between directions. That is, we choose, from the two antipodal eigenvectors, the one closer to the direction of the eigenvector of the mean susceptibility tensor.

2.4. Simulations

A total of 500 simulations have been run for each set of variables. The set of variables is constituted by the degree of anisotropy (P), the shape parameter (U), the standard deviation of the instrumental error distribution (σ) and the number of measurements (n).

Each variable constitutes a different piece of information in the final results. The standard deviation indicates how magnetically weak the data are, because σ is the ratio of the instrumental error to the mean susceptibility. The degree of anisotropy and the shape parameter indicate how anisotropically weak the data are. By increasing the number of measurements, the information about the instrumental error distribution and the statistical significance of the results are improved.

All the methods and simulations are implemented in R (free software programming language). The confidence level in all this study is set to 95%, being, therefore, $\alpha = 0.05$. The mean susceptibility λ_{mean} is taken as the unit of the susceptibility scale, so that the values of σ and the eigenvalues are dimensionless and to be understood as percentages of λ_{mean}. For the non-parametric bootstrap method, the repetition number N_b is set to 1000.

3. Results

A set of simulations have been performed to show how the reliability of the methods and their confidence intervals vary according to the ellipsoid parameters, the number of measurements and the instrumental error. The results are displayed in seven figures, each of them containing eight graphs. In each figure P and U are fixed and only the variable represented in the X-axis, either σ or n, varies while the other one remains also fixed. For each value of the X-axis variable, the plots in the eight graphs summarize the results of 500 simulations.

When σ varies, the value of n is fixed to $n = 20$, the threshold indicated by Tauxe (1998) to satisfy a confidence level of 95% in the non-parametric bootstrap. From these simulations we can determine a critical value, σ_c, that indicates the maximum σ for which both methods satisfy a 95% confidence level for $n = 20$. This σ_c is different for each set of values of P and U. When n varies, the value of σ is fixed to a chosen value higher than σ_c. The reason to run simulations varying n is to check if the reliability of the methods improves when the number of measurements increases.

The chosen combinations of P and U correspond to different types of ellipsoid. The values of P are 1.01 and 2, corresponding to a low anisotropy case and a high anisotropy case, respectively. The values of U are 0, 0.9 and −0.9, corresponding to a neutral, oblate and prolate ellipsoid, respectively, to study the behavior of the two end-members, the case with two close eigenvalues and the case with evenly spaced eigenvalues. We have not chosen the extreme values $U = \pm 1$, when two eigenvalues are equal, because speaking of confidence ellipses does not

make sense in that case since the eigenvector space would degenerate to a plane.

Mathematically there is no difference between choosing oblate or prolate ellipsoid, in both cases there are two eigenvalues very close to each other. Because of this, we have chosen an oblate ellipsoid ($U = 0.9$) for the case of low anisotropy ($P = 1.01$) and a prolate ellipsoid ($U = -0.9$) for the case of high anisotropy ($P = 2$).

All figures contain eight graphs distributed along two columns and four rows. The graphs in the left column represent in the Y-axis the percentage of successful results obtained by the two considered

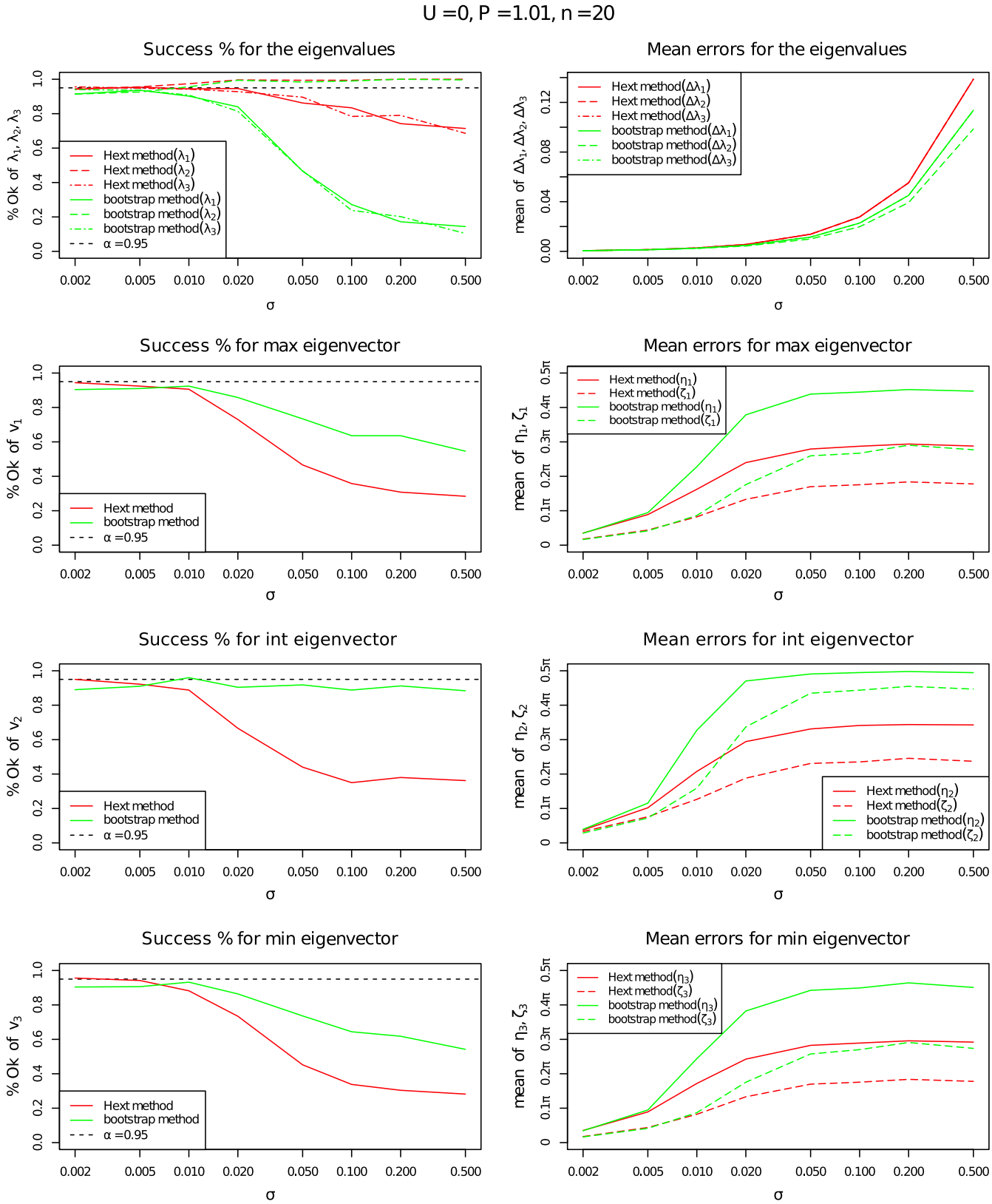

Fig. 1. Average mean errors of the eigenparameters and their reliability for $P = 1.01$, $U = 0$, and $n = 20$.

methods, with a dashed line indicating the 95% success. The first graph represents the success percentage in the estimation of the AMS eigenvalues λ_1, λ_2 and λ_3. The second, third and fourth graphs in the left side of the figure represent the success percentage in the estimation of the maximum, intermediate and minimum eigenvectors, $\mathbf{v}_1$, $\mathbf{v}_2$ and $\mathbf{v}_3$ respectively.

The graphs in the right column represent in the Y-axis the average size of the confidence intervals obtained by the two methods for a 95%

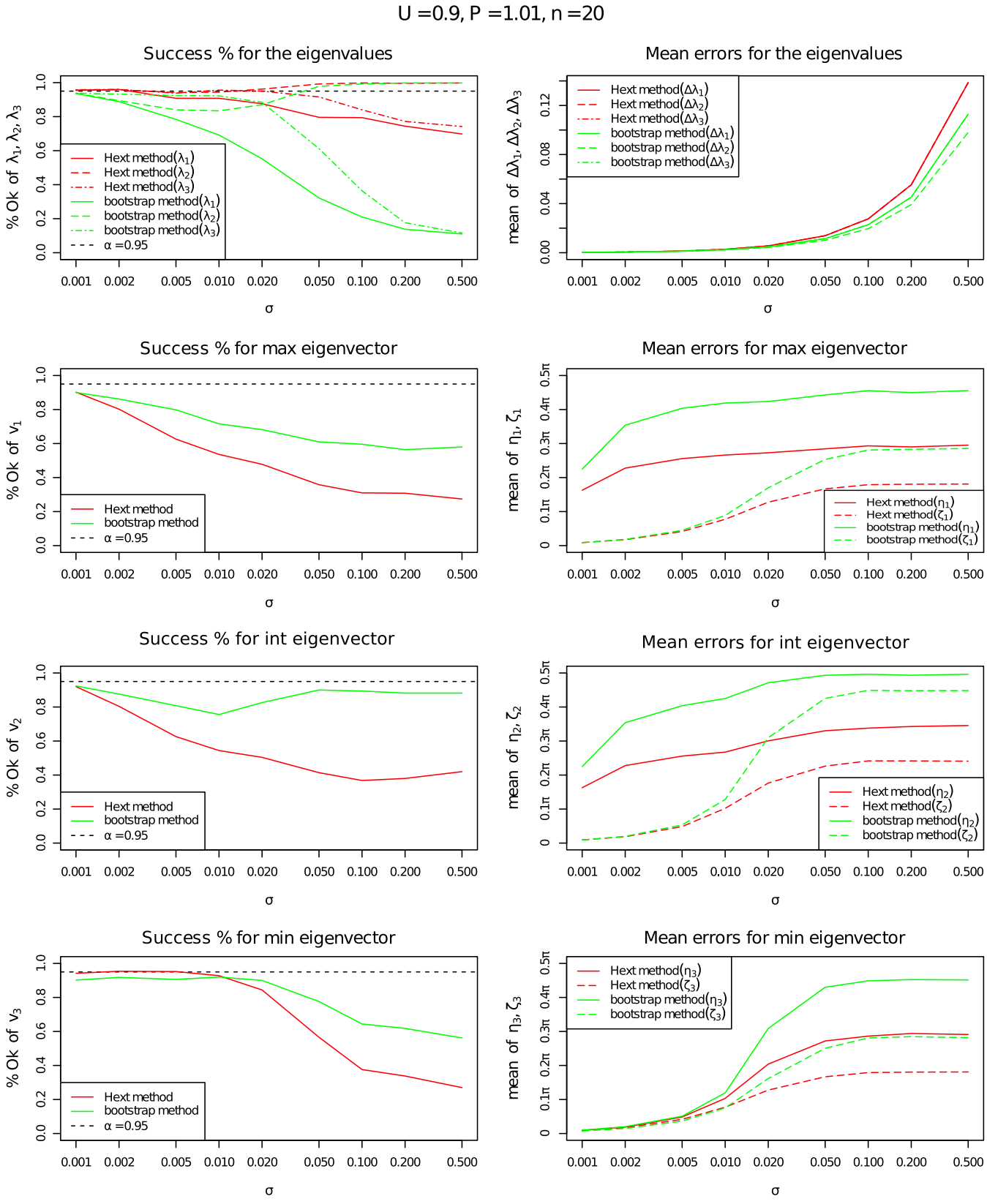

Fig. 2. Average mean errors of the eigenparameters and their reliability for $P = 1.01$, $U = 0.9$, and $n = 20$.

confidence level. The first graph shows the average confidence intervals of the eigenvalues, $\Delta\lambda_1$, $\Delta\lambda_2$ and $\Delta\lambda_3$. The second graph shows the mean semiaxes (semiangles) of the confidence ellipse for the maximum eigenvalue, η_1 (major semiaxis), ζ_1 (minor semiaxis), in radians. In the same way, the third and fourth graph show η_2, ζ_2, and η_3, ζ_3, for the intermediate and the minimum eigenvalue respectively.

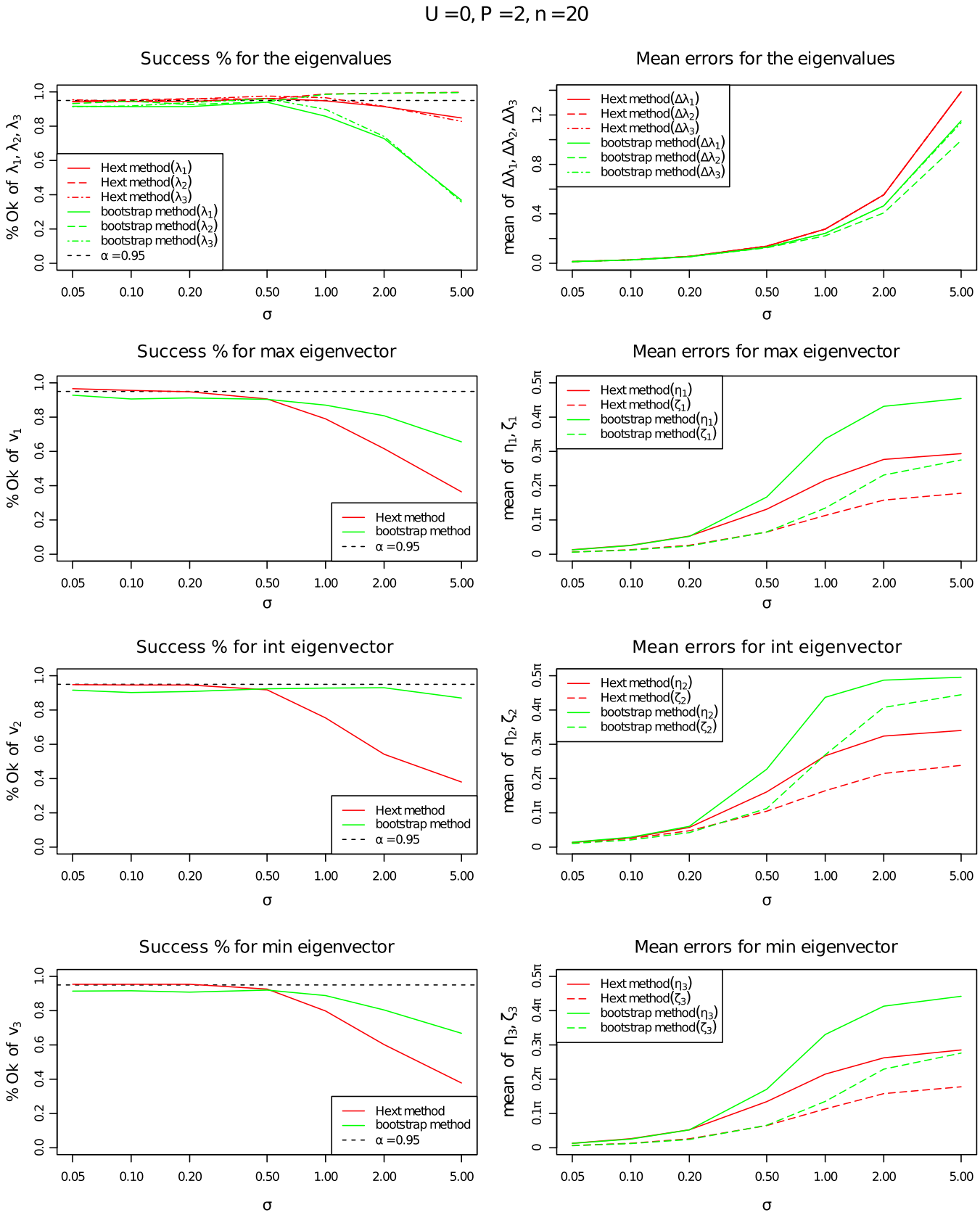

Fig. 3. Average mean errors of the eigenparameters and their reliability for $P = 2$, $U = 0$, and $n = 20$.

In Figs. 1, 2 and 3, the X-axis, in all graphs, represents σ, the standard deviation of the instrumental error distribution. In Figs. 4, 5, 6 and 7, the X-axis, in all graphs, represents n, the number of measurements.

3.1. Influence of σ

Fig. 1 summarizes the results of the experiment with a low anisotropy ($P = 1.01$) and neutral ellipsoid ($U = 0$) for $n = 20$. The

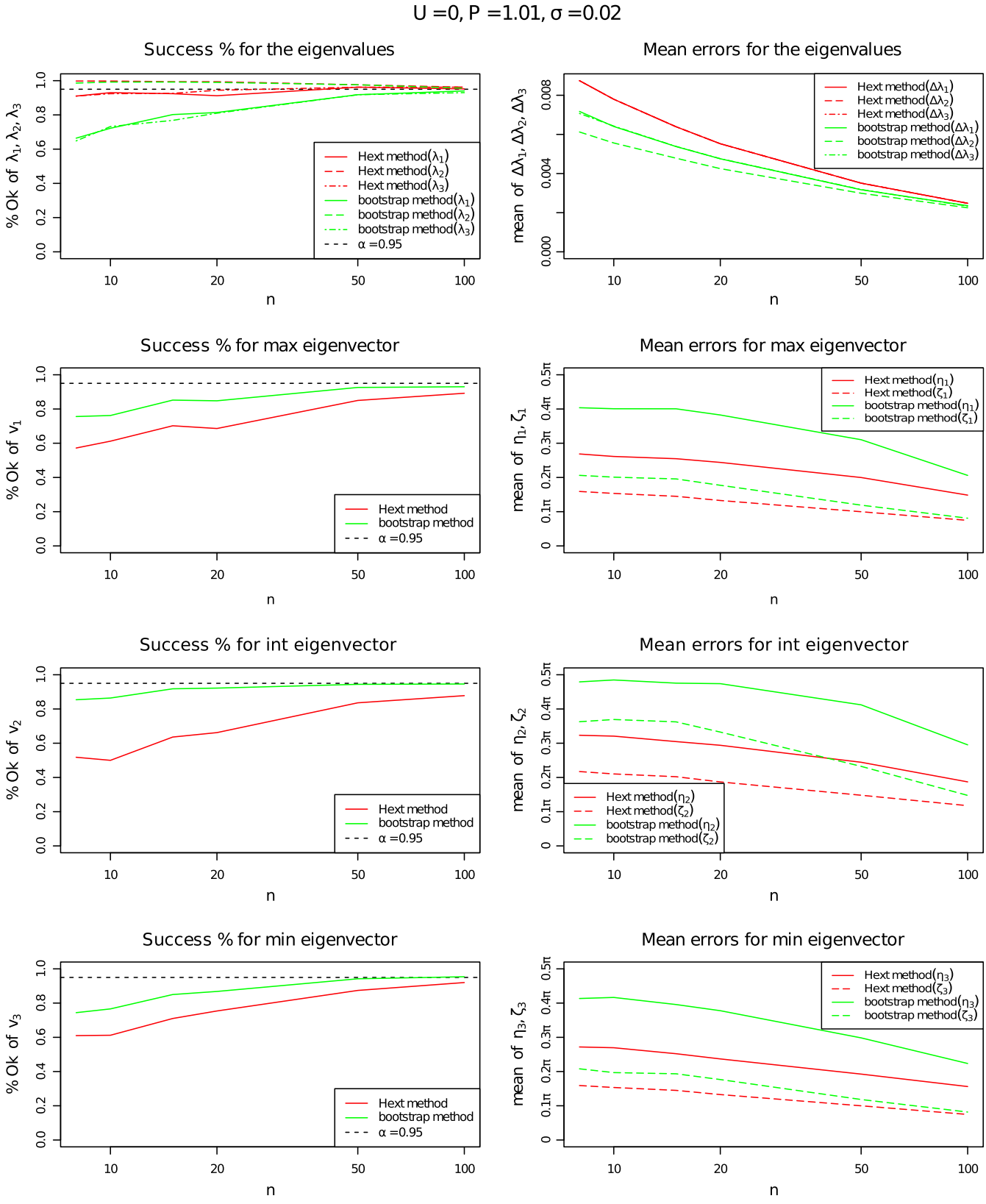

Fig. 4. Average mean errors of the eigenparameters and their reliability for $P = 1.01$, $U = 0$, and $\sigma = 0.02$.

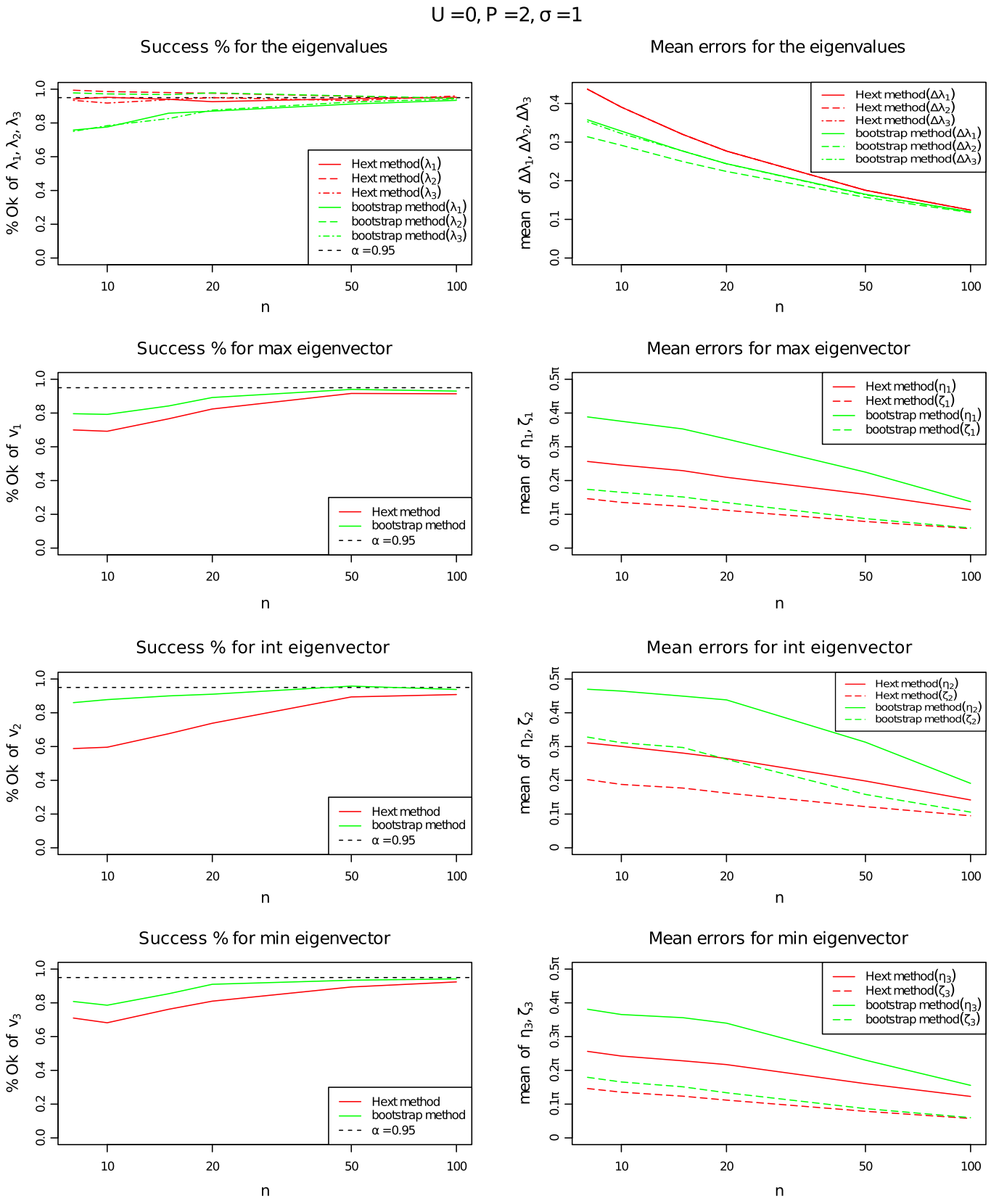

Fig. 5. Average mean errors of the eigenparameters and their reliability for $P = 2$, $U = 0$, and $\sigma = 1$.

differences between eigenvalues are 0.01, 1% of λ_{mean}. The value of σ_c, estimated from the graphs in the left column, is 0.005. This value of σ_c means that an instrumental error higher than 0.5% of λ_{mean} will provide a no reliable AMS ellipsoid for this set of values of P, U and n.

Fig. 2 corresponds to the example of low anisotropy and oblate ellipsoid for $n = 20$. The difference between eigenvalues is $\lambda_1 - \lambda_2 = 5 \cdot 10^{-4}$ [SI] and $\lambda_2 - \lambda_3 = 9.4 \cdot 10^{-3}$ [SI]. In this case, the value of σ_c is less than 0.001. The LPA method reaches a

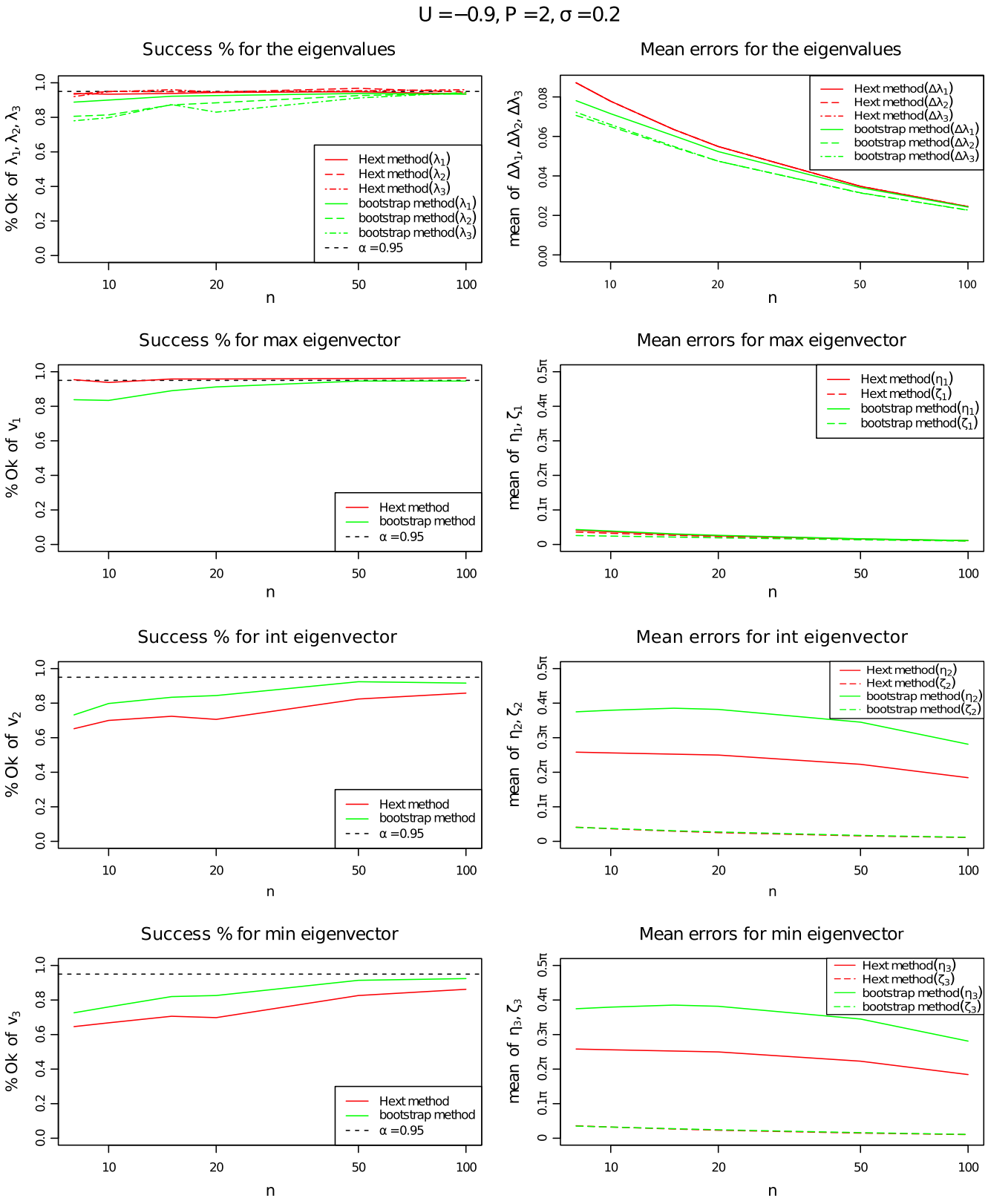

Fig. 6. Average mean errors of the eigenparameters and their reliability for $P = 2$, $U = -0.9$, and $\sigma = 0.2$.

confidence level of 95% for the eigenvalues and the eigenvector associated to the distinct eigenvalue (λ_3) for $\sigma = 0.01$, but not for the eigenvectors associated to the other eigenvalues. The NPB method only reaches a 95% confidence level for the eigenvalues for $\sigma = 0.001$.

Fig. 3 displays the results for a high anisotropy ($P = 2$) and neutral ellipsoid ($U = 0$) for $n = 20$. In this case, the value of σ_c is 0.2 and the differences between eigenvalues is 0.7.

Figs. 1, 2 and 3 show that σ has to be smaller than the differences between eigenvalues to be able to distinguish the eigenvalues and to make

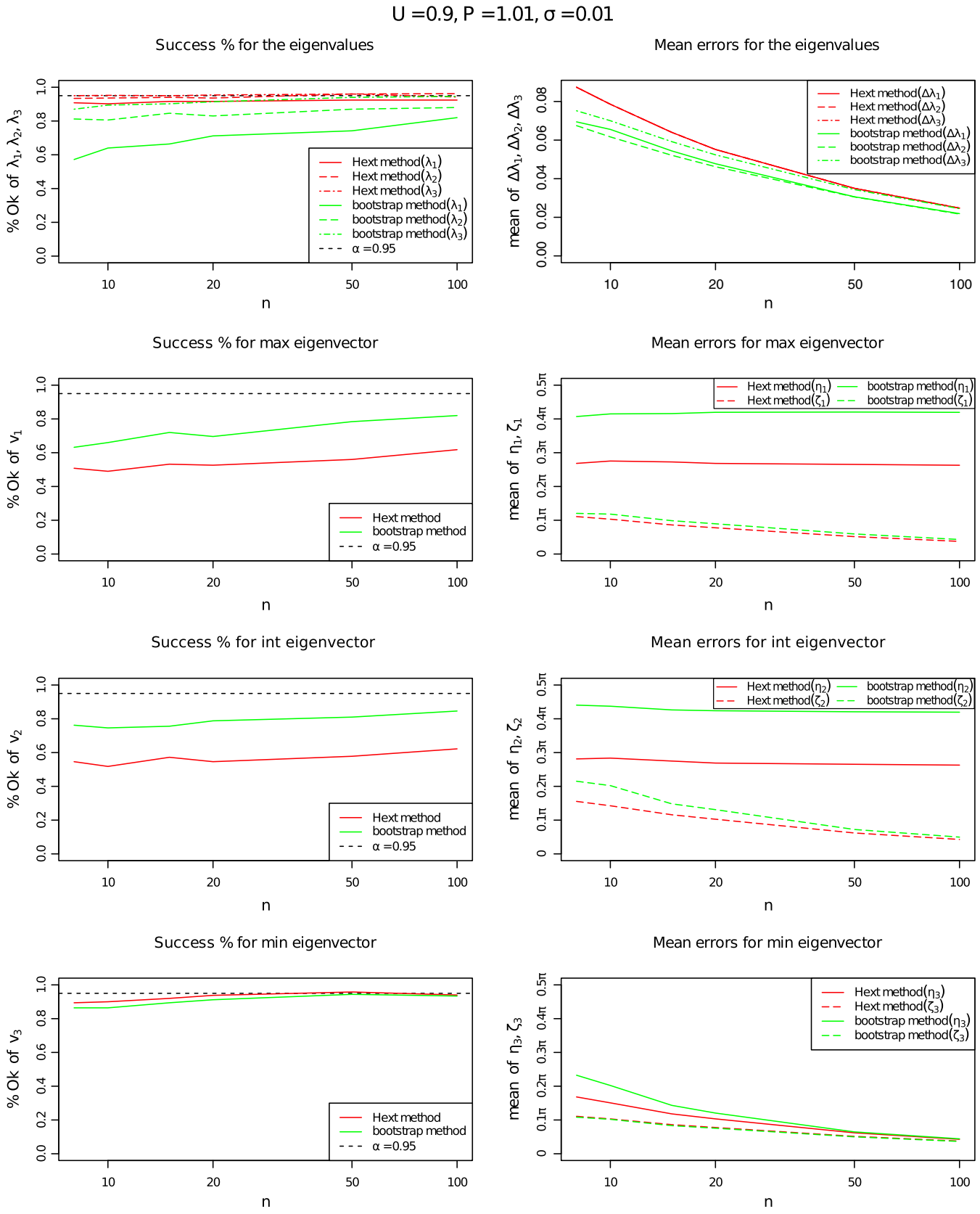

Fig. 7. Average mean errors of the eigenparameters and their reliability for $P = 1.01$, $U = 0.9$, and $\sigma = 0.01$.

a good interpretation of the principal directions. The range of reliability for both methods decreases (smaller σ_c) as the absolute value of the shape parameter increases and the anisotropy degree decreases. The results of the LPA and the NPB methods are much closer for $\sigma \leq \sigma_c$, both in the reliability and in the size of the confidence intervals. When the value of σ_c is exceeded, the negative slope in the eigenvector

reliability graphs of the LPA method is higher than the one in the NPB method, but the sizes of the NPB confidence intervals are much bigger, quickly approaching 90°. For the eigenvalues, the reverse behavior is observed, being the LPA method more reliable, without a big difference in the sizes of the confidence intervals, though. The case for $P = 2$, $U = -0.9$ and $n = 20$ is not shown in this paper because the trend is similar to the Figure 2, with a value of $\sigma_c = 0.05$.

3.2. Influence of n

In Figs. 4, 5, 6 and 7 we show how the reliability of the methods and the confidence intervals change when n increases for fixed values of P, U and σ. These graphs demonstrate that, by increasing the number of measurements, we can improve the reliability and minimize the AMS confidence intervals around half.

Fig. 4 shows the case of low anisotropy and neutral ellipsoid for a value of $\sigma = 0.02$, four times the value of σ_c. We can see that the NPB method needs $n \geq 50$ to reach a 95% confidence and the LPA method, $n \geq 100$. Fig. 5, the case of high anisotropy and neutral ellipsoid for a value of $\sigma = 1$, five times the value of σ_c, shows a critical value of $n = 50$ for both methods. Fig. 6 reflects the case of high anisotropy and prolate ellipsoid for a value of $\sigma = 0.2$, four times the value of σ_c. In this figure, the critical value of n for the eigenvalues is $n = 50$ for both methods, but for the eigenvectors, the NPB method needs $n = 50$ and the LPA method needs more than one hundred measurements.

In Fig. 7 we have simulated a case with $P = 1.01$, $U = 0.9$ and $\sigma = 0.01$, ten times the value of σ_c. A mineral with similar values of P and U is the quartz with $P = 1.01$ and $U = 1$ (Tarling and Hrouda, 1993). For quartz, with $k_{bulk} \sim 13.10^{-6}$ [SI], a value of $\sigma = 0.01$ would translate to an instrumental error of $1 \cdot 10^{-7}$ [SI]. This value can correspond to the total instrumental error for AGICO Instruments, since their sensitivity is in the range of 10^{-8} [SI] (Hrouda and Pokorný, 2011) and the total error is at least one order of magnitude larger than the sensitivity (Biedermann et al., 2013). For this case, only the LPA method can determine the eigenvalues with a 95% confidence level for the whole range of n (from 8 to 100). The NPB method cannot reach a 95% confidence level (for the eigenvalues) even with one hundred measurements. For the eigenvectors, no method can reach a 95% confidence level for the eigenvectors associated to the closest eigenvalues (Hall et al., 2009).

4. Discussion and conclusions

In this paper we have explored the well-resolved region for which the Linear Perturbation Analysis by Hext (1963) and the non-parametric bootstrap method proposed by Constable and Tauxe (1990) are reliable at a 95% confidence level. For that, we have performed simulations varying the ellipsoid parameters, P and U, the number of measurements n and the standard deviation of the instrumental error distribution, σ, taking as susceptibility unit the mean susceptibility λ_{mean}.

We have observed that the reliability of both methods depends on the ratio of instrumental error to mean susceptibility (magnetically weak samples) and the spacing of eigenvalues (anisotropically weak samples). For both methods there exists a maximum value of σ, named here critical value σ_c, for which the methods are reliable. This value of σ_c increases as the difference between eigenvalues does. That is, the value of σ_c is higher when the anisotropy degree increases and the shape parameter decreases. In order to reach the confidence level of 95% in both methods, the value of σ has to be smaller than the minimum difference between eigenvalues, at least for $n < 20$.

For fixed P and U, the confidence intervals are similar for both methods when they both are in their well-resolved region. When outside the well-resolved region, the behavior of both methods is different for the estimation of eigenvalues and their eigenvectors. For the eigenvalues, the success rate obtained by the LPA method is always higher than the one of the non-parametric bootstrap method, although the sizes of the eigenvalue errors of the LPA method are not much bigger. For the eigenvectors, the reverse is true. However, there is a big difference between the size of the errors (the semiangles obtained by the NPB method quickly overtake the value of 50°). Simulations reveal that when the methods are not reliable for a certain experimental setup (n, σ), the reliability region may be reached by sufficiently increasing n, resulting in considerably better accuracy too.

From these results we can suggest that when the eigenparameters are calculated by the two methods and the results are similar, then, they are in their well-resolved region and the results are reliable. But if there is a difference, the LPA method tends to be more reliable for the eigenvalues and the non-parametric bootstrap method for the eigenvectors, although the confidence ellipses may be too large for the results to be useful.

The current study can be used as an estimator of the measuring protocol for the evaluation of single crystal properties, where a previous estimation of the parameters (P, U, λ_{mean}) is available from theoretical calculations or preliminary measurements. From this previous estimation we can get an approximation of the spacing between eigenvalues ($\Delta\lambda$). Since the instrumental error distribution (and its σ) is part of the empirical method and cannot be changed significantly, the required number of measurements can be estimated before the actual measurement work is carried out. If $\sigma \leq \Delta\lambda/2$, $n = 20$ is enough to obtain reliable parameters. If $\sigma \sim \Delta\lambda$ it is necessary a value of $n = 50$. If $\sigma \geq 2\Delta\lambda$, n will reach unpractical values over one hundred measurements. The results presented in this work show the importance of the instrumental error distribution. This includes together with the technical instrumental sensitivity, additional sources of systematic errors related to the particular instrument and its location. It would be recommended for very precise determinations of AMS properties the evaluation of σ for each laboratory.

Acknowledgment

Authors are warmly grateful to G. Horcajada for helping with the development of the software and discussion. This paper has benefited significantly from two anonymous reviewer comments and Editor M. Jackson. Also Prof. A. M. Hirt is acknowledged for fruitful discussion. This work is supported by Project no CGL2011-24790 from Spanish Ministry of Economy and Competitiveness to SGS and a Ramon y Cajal contract to FMH.

Appendix A. Confidence ellipse calculation for the Kent distribution

According to Kent (1982), a $1-\alpha$ confidence ellipse can be obtained for the mean value $\overline{\mathbf{x}}$ of a set of vectors $\mathbf{x}_i$, with $i = 1 \ldots N_b$, that follow a Kent distribution. To obtain the ellipse parameters, the following steps are followed:

- calculate the mean vector $\overline{\mathbf{x}} = N_b^{-1} \sum \mathbf{x}_i$;
- calculate the dispersion matrix $\mathbf{S} = N_b^{-1} \sum \mathbf{x}_i \mathbf{x}_i^{\mathbf{T}}$;
- choose a rotation matrix $\mathbf{H}$ that rotates $\overline{\mathbf{x}}$ to the north polar axis, i.e.

$$\mathbf{H} = \begin{pmatrix} cos(\theta)cos(\phi) & -sin(\phi) & sin(\theta)cos(\phi) \\ cos(\theta)sin(\phi) & cos(\phi) & sin(\theta)sin(\phi) \\ -sin(\theta) & 0 & cos(\theta) \end{pmatrix}$$

where θ and ϕ are the polar coordinates of $\overline{\mathbf{x}}$;

- calculate the matrix $\mathbf{B} = \mathbf{H}^{\mathbf{T}}\mathbf{S}\mathbf{H}$;
- choose a rotation matrix $\mathbf{W}$ about the north pole to diagonalize the upper 2-by-2 submatrix of $\mathbf{B}$,

$$\mathbf{W} = \begin{pmatrix} cos(\psi) & -sin(\psi) & 0 \\ sin(\psi) & cos(\psi) & 0) \\ 0 & 0 & 1 \end{pmatrix}$$

- calculate the orientation matrix $\Gamma = \mathbf{HW}$, which is also a rotation;
- use Γ to transform the original vectors to the population standard frame of reference: $\mathbf{x}_i^* = \Gamma^{\mathbf{T}}\mathbf{x}_i$;
- in this standard frame of reference, with coordinates (x_1^*, x_2^*, x_3^*), the confidence ellipse's equation takes the form

$$N_b\mu^2\left(\frac{x_1^{*2}}{\sigma_1^2}+\frac{x_2^{*2}}{\sigma_2^2}\right)<\chi^2_{2;\alpha} \tag{4.1}$$

where $\chi^2_{2;\alpha}$ denotes the upper α critical value of the chi-squared distribution with 2 degrees of freedom, and

$$\mu = N_b^{-1}\sum x_{i3}^*, \sigma_1^2 = N_b^{-1}\sum x_{i1}^{*2}\sigma_2^2 = N_b^{-1}\sum x_{i2}^{*2};$$

- from Eq. (4.1), the major and minor semiaxes of the confidence ellipse are $\eta = arcsin\left(\sqrt{\frac{\sigma_1\chi^2_{2;\alpha}}{N_b\mu^2}}\right)$ and $\zeta = arcsin\left(\sqrt{\frac{\sigma_2\chi^2_{2;\alpha}}{N_b\mu^2}}\right)$, while the directions of the semiaxes are obtained from the two first columns of the orientation matrix Γ.

References

Biedermann, A.R., Lowrie, W., Hirt, A.M., 2013. A method for improving the measurement of low-field magnetic susceptibility anisotropy in weak samples. J. Appl. Geophys. 88, 122–130.

Borradaile, G.J., 2003. Statistics of Earth Science Data: Their Distribution in Time, Space and Orientation. Springer.

Borradaile, G., Henry, B., 1997. Tectonic applications of magnetic susceptibility and its anisotropy. Earth Sci. Rev. 42, 49–93.

Borradaile, G.J., Jackson, M., 2010. Structural geology, petrofabrics and magnetic fabrics (AMS, AARM, AIRM). J. Struct. Geol. 32, 1519–1551.

Borradaile, G.J., Stupavsky, M., Metsaranta, D.A., 2008. Induced magnetization of magnetite–titanomagnetite in alternating fields ranging from 400 a/m to 80,000 a/m; low-field susceptibility (100–400 a/m) and beyond. Pure Appl. Geophys. 165, 1411–1433.

Borradaile, G.J., Stupavsky, M., 1995. Anisotropy of magnetic susceptibility: Measurement schemes. Geophys. Res. Lett. 22, 1957–1960.

Cañón-Tapia, E., Walker, G.P., Herrero-Bervera, E., 1995. Magnetic fabric and flow direction in basaltic pahoehoe lava of xitle volcano, Mexico. J. Volcanol. Geotherm. Res. 65, 249–263.

Constable, C., Tauxe, L., 1990. The bootstrap for magnetic susceptibility tensors. J. Geophys. Res. Solid Earth 95, 8383–8395 (1978–2012).

Davison, A.C., 1997. Bootstrap methods and their application, Volume 1. Cambridge University Press.

Dunlop, D.J., Özdemir, Ö., 2001. Rock magnetism: fundamentals and frontiers, Volume 3. Cambridge University Press.

Ernst, R.E., Baragar, W., 1992. Evidence from magnetic fabric for the flow pattern of magma in the Mackenzie giant radiating dyke swarm. Nature 356, 511–513.

Hall, P., L, Y.K., P, B.U., P, D., 2009. Tie-respecting bootstrap methods for estimating distributions of sets and functions of eigenvalues. Bernoulli 15, 380–401.

Hamilton, N., Rees, A., 1970. The use of magnetic fabric in paleocurrent estimation. Palaeogeophysics 445–464.

Hext, G.R., 1963. The estimation of second-order tensors, with related tests and designs. Biometrika 50, 353–373.

Hrouda, F., 1993. Theoretical models of magnetic anisotropy to strain relationship revisited. Phys. Earth Planet. Inter. 77, 237–249.

Hrouda, F., 2002. Low-field variation of magnetic susceptibility and its effect on the anisotropy of magnetic susceptibility of rocks. Geophys. J. Int. 150, 715–723.

Hrouda, F., Pokornỳ, J., 2011. Extremely high demands for measurement accuracy in precise determination of frequency-dependent magnetic susceptibility of rocks and soils. Stud. Geophys. Geod. 55, 667–681.

Jelinek, V., 1977. The statistical theory of measuring anisotropy of magnetic susceptibility of rocks and its application. Geoflz. Brno 87.

Jelínek, V., 1978. Statistical processing of anisotropy of magnetic susceptibility measured on groups of specimens. Stud. Geophys. Geod. 22, 50–62.

Jelinek, V., 1981. Characterization of the magnetic fabric of rocks. Tectonophysics 79, T63–T67.

Kent, J.T., 1982. The Fisher–Bingham distribution on the sphere. J. R. Stat. Soc. Ser. B Methodol. 71–80.

Kodama, K.P., 1995. Magnetic fabrics. Rev. Geophys. 33, 129–135.

Nagata, T., 1961. Rock Magnetism. Maruzen Company, Tokyo.

Owens, W., 2000a. Statistical analysis of normalized and unnormalized second-rank tensor data, with application to measurements of anisotropy of magnetic susceptibility. Geophys. Res. Lett. 27, 2985–2988.

Owens, W., 2000b. Statistical applications to second-rank tensors in magnetic fabric analysis. Geophys. J. Int. 142, 527–538.

Rochette, P., Jackson, M., Aubourg, C., 1992. Rock magnetism and the interpretation of anisotropy of magnetic susceptibility. Rev. Geophys. 30, 209–226.

Schmidt, V., Günther, D., Hirt, A.M., 2006. Magnetic anisotropy of calcite at room-temperature. Tectonophysics 418, 63–73.

Tarling, D., Hrouda, F., 1993. Magnetic Anisotropy of Rocks. Springer.

Tauxe, L., 1998. Paleomagnetic Principles and Practice. Number 17 in Modern Approaches in Geophysics. Kluwer Academic Publishers, Dordrecht; Boston.

Tauxe, L., 2010. Essentials of Paleomagnetism. University of California Press, Berkeley.

Werner, T., 1997. Experimental designs for determination of the anisotropy of remanence-test of the efficiency of least-square and bootstrap methods applied to metamorphic rocks from southern Poland. Phys. Chem. Earth 22, 131–136.